J Electroceram (2006) 16: 141–149
DOI 10.1007/s10832-006-4927-2

Dielectric properties and morphotropic phase boundaries in the $x\mathrm{Pb}(\mathrm{Zn}_{1/3}\mathrm{Nb}_{2/3})\mathrm{O}_3-(1-x)\mathrm{Pb}(\mathrm{Zr}_{0.5}\mathrm{Ti}_{0.5})\mathrm{O}_3$ pseudo-binary system

N. Vittayakorn · G. Rujijanagul · X. Tan · H. He · M. A. Marquardt · D. P. Cann

Received: 24 June 2004 / Revised: 15 April 2005 / Accepted: 9 September 2005

Abstract Ceramics in the $x\mathrm{Pb}(\mathrm{Zn}_{1/3}\mathrm{Nb}_{2/3})\mathrm{O}_3-(1-x)\mathrm{Pb}(\mathrm{Zr}_{0.5}\mathrm{Ti}_{0.5})\mathrm{O}_3$ [xPZN–$(1-x)$PZT] solid solution system are expected to display excellent dielectric, piezoelectric, and ferroelectric properties in compositions close to the morphotropic phase boundary (MPB). The dielectric behavior of ceramics with $x = 0.1-0.6$ has been characterized in order to identify the MPB compositions in this system. Combined with X-ray diffraction results, ferroelectric hysteresis measurements, and Raman reflectivity analysis, it was consistently shown that an MPB exists between $x = 0.2$ and $x = 0.3$ in this binary system. When $x \leq 0.2$, the tetragonal phase dominates at ambient temperatures. In the range of $x \geq 0.3$, the rhombohedral phase dominates. For this rhombohedral phase, electrical measurements reveal a profound frequency dispersion in the dielectric response when $x \geq 0.6$, suggesting a transition from normal ferroelectric to relaxor ferroelectric between $0.5 \leq x \leq 0.6$. Excellent piezoelectric properties were found in 0.3PZN–0.7PZT, the composition closest to the MPB with a rhombohedral structure. The results are summarized in a PZN–PZT binary phase diagram.

N. Vittayakorn (✉)
Department of Chemistry, Faculty of Science, King Mongkut's Institute of Technology, Ladkabang, Bangkok, 10520, Thailand

G. Rujijanagul
Department of Physics, Faculty of Science, Chiang Mai University, Chiang Mai 50200, Thailand

X. Tan · H. He · M. A. Marquardt
Materials Science and Engineering Department, Iowa State University, Ames, IA 50011, USA

David P. Cann
Department of Mechanical Engineering, Oregon State University, Corvallis, OR 97331, USA

1. Introduction

Piezoelectric materials are widely used for various devices, including multilayer capacitors, sensors, and actuators. By the 1950's, the ferroelectric solid solution $\mathrm{Pb}(\mathrm{Zr}_{1-x}\mathrm{Ti}_x)\mathrm{O}_3$ (PZT) was found to host exceptionally high dielectric and piezoelectric properties for compositions close to the morphotropic phase boundary (MPB). This MPB is located around $\mathrm{PbZrO_3}$:$\mathrm{PbTiO_3} \sim 0.52$:0.48 and separates a Ti-rich tetragonal phase from a Zr-rich rhombohedral phase [1]. Most commercial PZT ceramics are thus designed in the vicinity of the MPB with various dopings in order to achieve optimum properties. It is interesting to notice that recent high resolution structure studies have revealed that the morphotropic phase boundary spans a narrow composition range where the solid solution displays a monoclinic symmetry. The intermediate monoclinic phase bridges the rhombohedral to tetragonal phase transition [2–4].

$\mathrm{Pb}(\mathrm{Zn}_{1/3}\mathrm{Nb}_{2/3})\mathrm{O}_3$ (PZN) is an important relaxor ferroelectric material with the rhombohedral structure at room temperature. A diffuse phase transition from the paraelectric state to a ferroelectric polar state occurs at 140°C [5]. Extensive research has been carried out on PZN single crystals because of their excellent dielectric, electrostrictive, and optical properties [6]. Although single crystals of PZN can routinely be grown by the flux method [7], it is known that perovskite PZN ceramics cannot be synthesized by the conventional mixed-oxide method without doping [8]. Attempts to synthesize perovskite PZN ceramics invariably results in the formation of a pyrochlore phase with accompanying degradation of the dielectric and piezoelectric properties. Various chemical additives, such as $\mathrm{Ba}(\mathrm{Zn}_{1/3}\mathrm{Nb}_{2/3})\mathrm{O}_3$, $\mathrm{BaTiO_3}$, and $\mathrm{SrTiO_3}$ have thus been explored in an attempt to stabilize the perovskite PZN ceramic [9, 10]. However, a trade-off is made with these additives leading to reduced dielectric constants

and piezoelectric coefficients. Therefore, there is significant interest in finding a method to stabilize the perovskite phase in PZN without sacrificing the excellent dielectric and piezoelectric properties.

Recent work has shown that ultrahigh piezoelectric properties can be obtained in relaxor-normal ferroelectric solid solutions with compositions close to the MPB, such as the $Pb(Mg_{1/3}Nb_{2/3})O_3$–$PbTiO_3$ system and the $Pb(Zn_{1/3}Nb_{2/3})O_3$–$PbTiO_3$ system [6, 11]. Since both PZT and PZN have the perovskite structure and both are known to have excellent dielectric and piezoelectric properties, one approach to stabilize and optimize PZN ceramics is to alloy PZN with PZT. Fan et al. [12] have successfully produced phase-pure perovskite of $xPb(Zn_{1/3}Nb_{2/3})O_3 - (1 - x)Pb(Zr_{0.47}Ti_{0.53})O_3$ ceramics in the range of $0.4 \leq x \leq 0.7$ via the conventional mixed-oxide method and observed excellent properties near the MPB composition. In our previous work, we compared the conventional mixed-oxide method with the columbite method in the preparation of a similar system $xPb(Zn_{1/3}Nb_{2/3})O_3-(1 - x)Pb(Zr_{0.5}Ti_{0.5})O_3$ [xPZN–$(1 - x)$PZT] and found that the columbite method leads to better compositional homogeneity and ferroelectric properties [13]. The present work aims to provide further information on the dielectric and piezoelectric properties and phase transitions in this xPZN–$(1 - x)$PZT binary system prepared by both methods, with the purpose of confirming improved properties in ceramics synthesized via the columbite method.

2. Experimental procedure

For the conventional method, regent grade oxides of PbO, ZnO, ZrO_2, TiO_2 and Nb_2O_5 were mixed in the required stoichiometric ratios for the general composition xPZN–$(1 - x)$PZT where x = 0.1, 0.2, 0.3, 0.4, 0.5 and 0.6. An additional 2 mol% excess PbO was added to account for PbO volatility. After ball milling for 24 hours and drying at 120°C, the mixture was calcined at temperatures between 750 to 950°C for 4 hours using a double crucible configuration [14]. A heating rate of 20°C/min was selected for all of the compositions in this system. For the columbite method, the columbite precursor $ZnNb_2O_6$ was prepared from the reaction between ZnO (99.9%) and Nb_2O_5(99.9%) at 975°C for 4 hours. The wolframite precursor $ZrTiO_4$ was formed by reacting ZrO_2(99.9%) with TiO_2(99.9%) at 1400°C for 4 hours. The precursors $ZnNb_2O_6$, $ZrTiO_4$ were then mixed with PbO (99.9%) according to the stoichiometric ratio for the desired compositions with 2 mol% excess PbO added. The mixtures were then followed the same processing conditions as the conventional method. To minimize the influence of grain size effects, the calcined powders from both processing methods were ball-milled for 24 hours and dried at 120°C. The calcined powders were cold isostatically pressed into pellets at a pressure of 150 MPa. A total of four sintering conditions were utilized: 1150°C, 1200°C, 1225°C, 1250°C, all with a dwell time of 2 hours. To inhibit PbO volatilization from the pellets, a PbO atmosphere was maintained with a bed of $PbZrO_3$ powder placed in the vicinity of the pellets. The calcined powder and sintered pellets were checked for perovskite phase formation by X-ray diffraction (XRD).

Thin slices cut from sintered pellets were prepared with sputtered gold electrodes for electrical characterization. The relative permittivity (ε_r) was measured with an LCR meter (HP-4284A, Hewlett-Packard Inc.) at frequencies of 0.1, 1, 10, and 100 kHz in conjunction with an environmental chamber with a temperature range of 25–450°C. A heating rate of 3°C/min was used during measurements. The piezoelectric coefficient (d_{33}) was measured with a d_{33} meter (Model 8000 d_{33} Tester) on poled slices. The electromechanical coupling factor (k_p) was calculated according to the resonance and anti-resonance frequencies obtained with an impedance analyzer (Model 4194A, HP).

Raman scattering was measured on polished specimens using a Renishaw in Via Reflex Raman spectrometer with a 488 nm radiation source. The grain size was evaluated by scanning electron microscopy (SEM) (JSM5410, JEOL) and the ferroelectric domain morphology was examined by transmission electron microscopy (TEM) (CM30, Phillips).

3. Results and discussion

3.1. Perovskite phase formation

Powder XRD was extensively used to monitor the phase development at each step during ceramic preparation to ensure the phase purity. Phase-pure precursors $ZnNb_2O_6$ and $ZrTiO_4$ were obtained using the calcination conditions described previously. The calcined powders for the perovskite solid solutions were also examined by XRD and the results are exemplified by the powders of 0.5PZN–0.5PZT, as shown in Fig. 1. Similar trends were apparent for both the conventional method and the columbite method: higher calcination temperatures led to higher perovskite phase purity. At 900°C, the pyrochlore phase disappeared below the resolution limits of X-ray diffraction.

The perovskite phase development at different calcination temperatures was estimated from the X-ray diffraction data with the commonly used formula [15]:

$$\text{Perovskite } \% = \left(\frac{I_{\text{perov}}}{I_{\text{perov}} + I_{\text{pyro}} + I_{\text{PbO}}} \right) \times 100 \qquad (1)$$

where I_{perov}, I_{pyro}, and I_{PbO} refer to the intensity of the (110) perovskite peak, (222) pyrochlore peak, and the intensity of the highest PbO peak, respectively. The calculation for the data shown in Fig. 1 for the 0.5PZN–0.5PZT powder is plotted in Fig. 2, where the peak intensity ratio illustrates the evolution of phase-pure perovskite. The increase in the

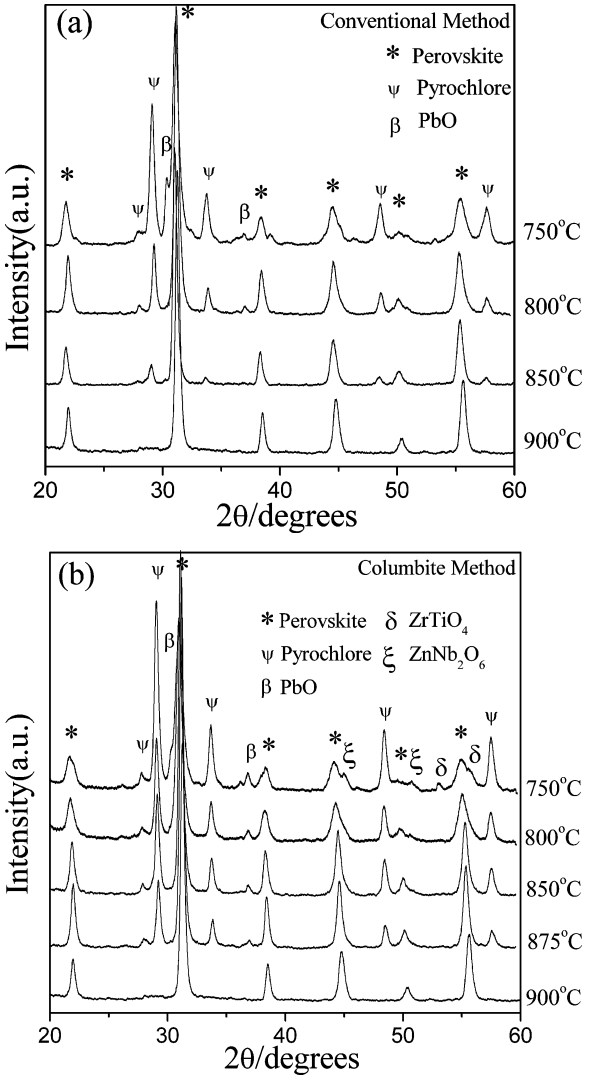

Fig. 1 XRD spectra of 0.5PZN–0.5PZT powder calcined at various temperatures for 4 hours. (a) The conventional mixed-oxide method; and (b) the columbite method

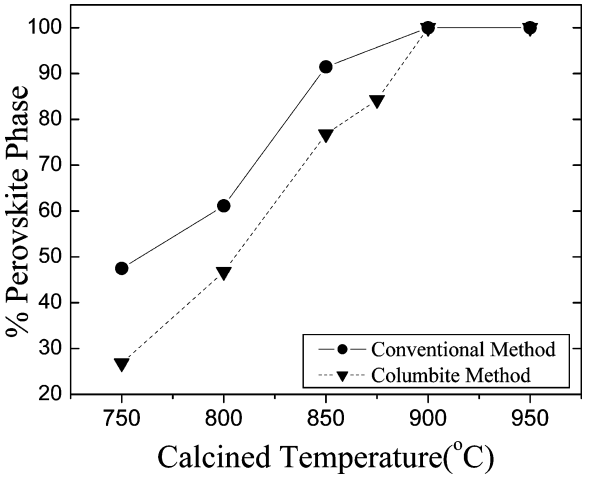

Fig. 2 Perovskite phase content in 0.5PZN–0.5PZT powders calcined at different temperatures

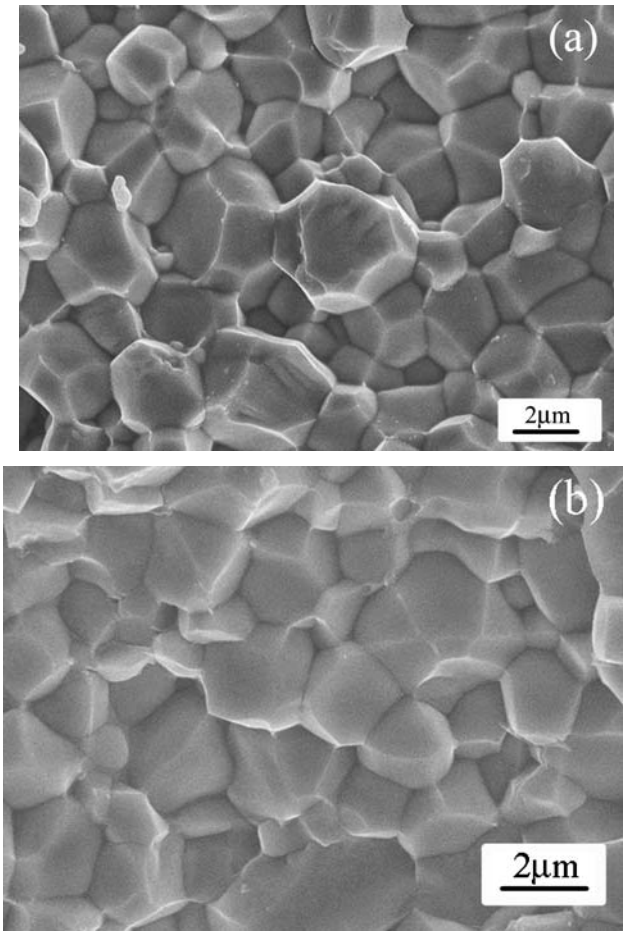

Fig. 3 SEM examination of the grain morphology in 0.5PZN–0.5PZT ceramics sintered at 1225°C for 2 hours: (a) conventional method; and (b) columbite method

phase purity with increasing calcination temperature for both methods is evident. It is noted in Fig. 2 that the conventional method showed a higher amount of the perovskite phase than the columbite method below 900°C. Presumably the difference is due to the different reaction paths between the two methods.

After sintering of the powders calcined at 900°C, the perovskite phase was preserved as evidenced by XRD with one exception. At the highest PZN concentration of $x = 0.6$, a small amount of pyrochlore phase was detected though the sample remained approximately 98.5% perovskite.

The sintered pellets appeared to be dense and the grain size was in the range of 1–5 μm, as shown in Fig. 3. The comparison between Figs. 3(a) and (b) indicates that the conventional method produces ceramics with slightly coarser grains.

3.2. Dielectric behavior

The relative permittivity of xPZN–$(1-x)$PZT ceramics was measured as a function of temperature up to 450°C at different frequencies. The results are presented in Fig. 4 for

Table 1 Comparison of the dielectric properties of xPZN–$(1-x)$PZT ceramics prepared by the conventional mixed-oxide and columbite methods

x	T_{max}(°C)		ε_r at 25°C		ε_r at T_{max}	
	Conventional	Columbite	Conventional	Columbite	Conventional	Columbite
$x = 0.1$	359	351	810	1,590	13,300	21,200
$x = 0.2$	329	324	1,230	1,550	25,000	25,800
$x = 0.3$	309	299	980	1,580	14,300	15,700
$x = 0.4$	281	273	1,230	1,440	17,000	20,800
$x = 0.5$	250	242	1,220	1,430	20,800	21,200
$x = 0.6$	240	231	1,230	1,440	11,400	13,200

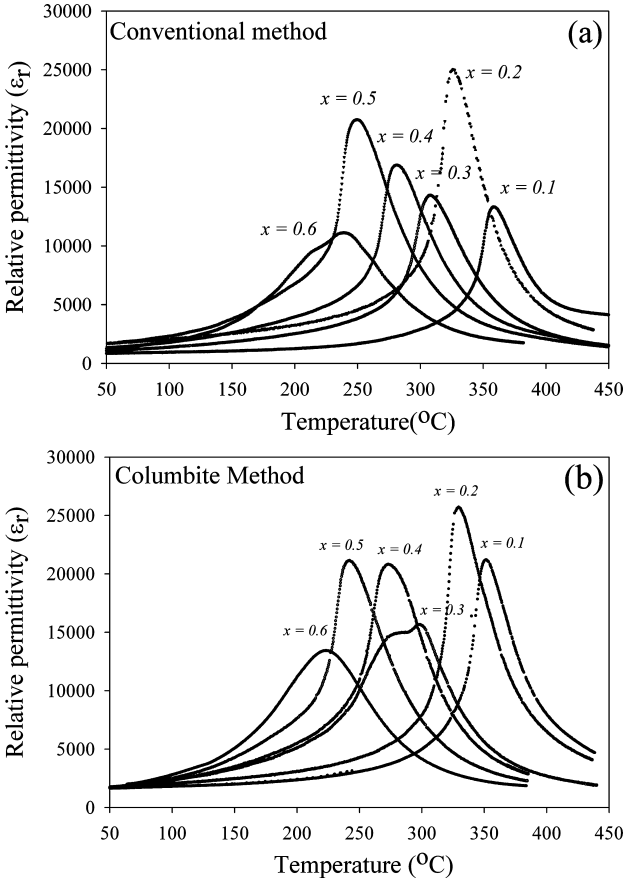

Fig. 4 Relative permittivity versus temperature curves for the xPZN$-(1-x)$PZT ceramics sintered at 1250°C for $x = 0.1$ and 0.2 and sintered at 1225°C for $x = 0.3$-0.6 for 2 hours. The frequency used for the measurement is 1 kHz: (a) conventional method; and (b) columbite method

ceramics prepared by the two methods. It is interesting to note that all compositions show a dispersive dielectric behavior with respect to frequency. However, the frequency dispersion in the PZN–PZT binary system is not as strong as that in the pure relaxor PZN. For all compositions, Table 1 lists the temperature at which the permittivity is maximum (T_{max}), and the relative permittivity both at room temperature and at T_{max}. These results show that the permittivity of ceramics prepared via the columbite method was significantly higher than that of ceramics synthesized by the conventional method. It is also evident from Fig. 4 and Table 1 that 0.2PZN–0.8PZT and 0.5PZN–0.5PZT show the highest peak values of the relative permittivity. For the 0.2PZN–0.8PZT composition, the peak value reads 25,800 for the columbite method and 25,000 for the conventional method. For the 0.5PZN–0.5PZT composition, the peak relative permittivity is 21,200 for the columbite method and 20,800 for the conventional method.

The ε_r versus T curves shown in Fig. 4 are also indicative of thermally induced phase transitions. These transitions are prominent in the compositions $x = 0.3$, 0.5 and 0.6 as depicted separately in Figs. 5(a), (b), and (c). At the composition $x = 0.3$ two peaks were revealed at temperatures 283.6°C and 298.8°C in the ceramic prepared by the columbite method (Fig. 5(a)). However, this was not observed in ceramics of the same composition prepared via the conventional method. In this case, there was only one peak present at 309°C. These two peaks are believed to be due to the phase transitions, as will be further explained later. We argue that the columbite method produces ceramics with better compositional homogeneity than the conventional mixed oxide method. In the ceramics prepared by the conventional method, due to compositional fluctuations the two transitions were obscured.

For the composition $x = 0.5$, the ε_r versus T curves revealed the occurrence of transitions between normal ferroelectric and relaxor ferroelectric behaviors, as indicated in Fig. 5(b). These transitions were observed in ceramics prepared by both methods. In Fig. 5(b) which shows the dielectric behavior of the ceramic prepared via the columbite method, a strong frequency dispersion in the permittivity was evident at temperatures T > 242°C and T < 235°C. In the narrow temperature range of 235°C < T < 242°C, the permittivity increased precipitously. This temperature range is bounded by $T_{startNR}$ and $T_{finishNR}$, as denoted in Fig. 5(b). The subscript NR stands for the normal ferroelectric↔relaxor ferroelectric transition. Similar transitions have been observed by other researchers in other solid solution systems [16] The $x = 0.6$ composition showed a broadening of the permittivity maxima and T_m increased with increasing measurement frequency (Fig. 5(c)). This indicates that this composition shows

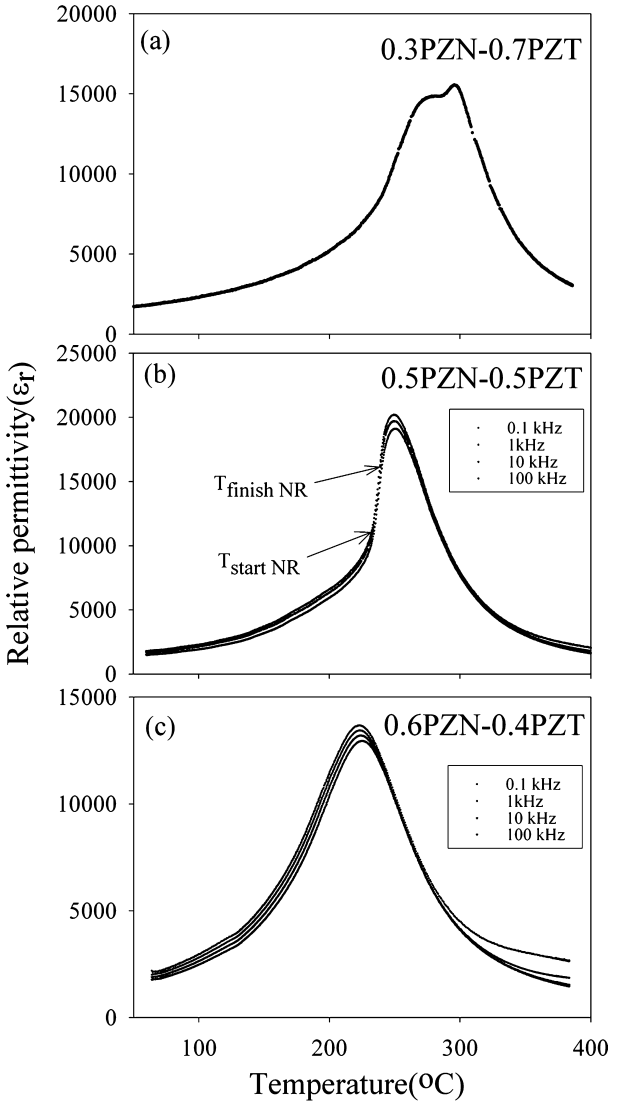

Fig. 5 Phase transitions detected from the ε_r versus T curves in ceramics prepared via the columbite method and sintered at 1225°C for 2 hours. (a) 0.3PZN–0.7PZT ceramic at 1 kHz; and (b) 0.5PZN–0.5PZT ceramic at 0.1, 1, 10 and 100 kHz. (c) 0.6PZN–0.4PZT ceramic at 0.1, 1, 10 and 100 kHz

a diffuse phase transition with a strong frequency dispersion which is characteristic of relaxor ferroelectricity.

Figure 5 also shows that an increase in PZN mole fraction leads to a decrease in $T_{\max}$. The variation in transition temperature with composition is detailed in Fig. 6. The ceramics produced by the columbite method show a slightly lower transition temperature compared to ceramics produced by the conventional method. A quasi-linear relationship between $T_{\max}$ and x is evident. This linear relation follows closely to the rule of mixtures, as expressed by:

$$T_{\max} = x(140^{\circ}\mathrm{C}) + (1-x)(390^{\circ}\mathrm{C}) \tag{2}$$

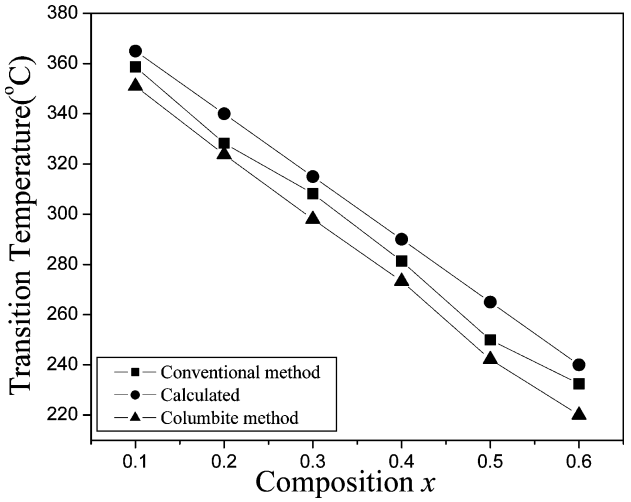

Fig. 6 Variation of $T_{\max}$ with increasing PZN content x in the xPZN–$(1-x)$PZT system. $T_{\max}$ is measured from Fig. 4

where 140°C and 390°C are the $T_{\max}$ values for the two constituent compounds PZN and PZT, respectively. From Fig. 6, the calculated $T_{\max}$ from Eq. (2) is slightly higher than the actual transition temperature.

Above $T_{\max}$, the ε_r versus T curve for a normal ferroelectric can be described by the Curie-Weiss law:

$$\frac{1}{\varepsilon_r} = \frac{T-\theta}{C} \tag{3}$$

where θ is the Curie-Weiss temperature and C is the Curie constant. When a normal ferroelectric forms a solid solution with a relaxor, the ε_r versus T relationship follows a similar function with additional variables γ and δ_γ: [17].

$$\frac{\varepsilon'_m}{\varepsilon'(f,T)} = 1 + \frac{(T-T_m(f))^{\gamma}}{2\delta_\gamma^2} \tag{4}$$

where $1 \le \gamma \le 2$. When $\gamma = 1$, Eq. (4) becomes the Curie-Weiss law; when $\gamma = 2$ this equation describes the ideal relaxor behavior with a quadratic dependence. The parameter ε'_m is the peak permittivity at $T = T_m(f)$and δ_γ is a parameter which describes the degree of diffuseness of the phase transition. The parameters γ and δ_γ are both material constants which depend on the composition and structure.

Plots of $\log[(\varepsilon_m/\varepsilon)-1]$ vs. $\log(T-T_m)$ for $x = 0.1$ and 0.5 are shown in Fig. 7 where linear relationships can be clearly seen. The parameter γ is determined to be 1.34 and 1.71 and the diffusiveness parameter δ_γ is measured to be 10.7 and 16.7 in ceramics prepared with the columbite method for $x = 0.1$ and 0.5, respectively. As the PZN mole fraction increases, the solid solution displays more relaxor-like characteristics.

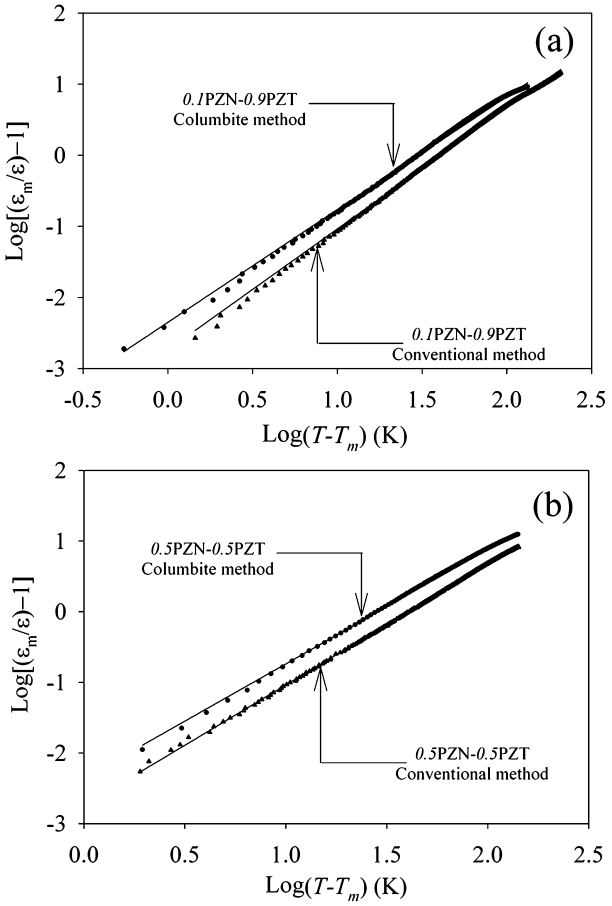

Fig. 7 The $\log[(\frac{\varepsilon_{r\max}}{\varepsilon}) - 1]$ vs. $\log(T - T_{\max})$ plots for (a) 0.1PZN–0.9PZT and (b) 0.5PZN–0.5PZT ceramics from data shown in Fig. 4

3.3. The morphotropic phase boundary

On the basis of XRD and ferroelectric hysteresis measurements, we have identified the MPB in the $x\text{Pb}(\text{Zn}_{1/3}\text{Nb}_{2/3})\text{O}_3 - (1-x)\text{Pb}(\text{Zr}_{0.5}\text{Ti}_{0.5})\text{O}_3$ system in our previous work [13]. The MPB sits between $x = 0.2$ and $x = 0.3$, separating the tetragonal phase for $x \leq 0.2$ from the rhombohedral phase for $x \geq 0.3$. This MPB is also confirmed by the dielectric data shown in Fig. 4, where the maximum permittivity $\varepsilon_{r\max}$ shows a peak at $x = 0.2$. Figure 8 replots the $\varepsilon_{r\max}$ *vs.* x in our xPZN–$(1-x)$PZT system, together with the results from our previous coercive field measurements.

In addition to the MPB that separates the tetragonal from the rhombohedral phase, there is another transition from normal ferroelectric to relaxor ferroelectric for the rhombohedral phase. Compared to the tetragonal-to-rhombohedral structural transition, this ferroelectric transition is more gradual. However, for the composition of $x = 0.6$ characteristic relaxor ferroelectric behavior is evident, as indicated by the profound dispersion in the dielectric response (Fig. 5(c)). Although this ferroelectric transition is not reflected in the E_C measurements, the relative permittivity clearly shows a

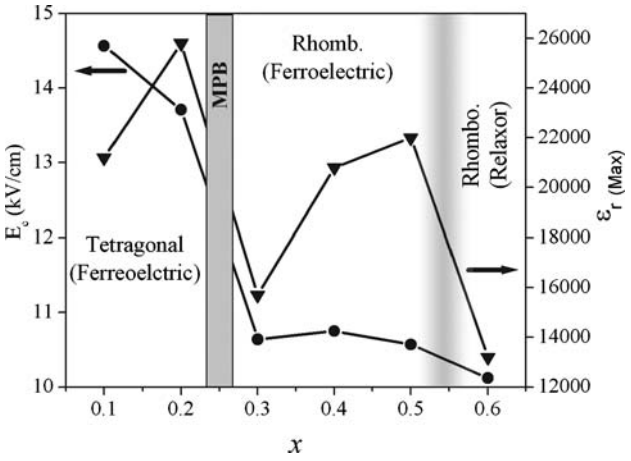

Fig. 8 Coercive field (E_c) and peak relative permittivity versus x in xPZN-$(1-x)$PZT ceramics showing the presence of MPB at x between 0.2 and 0.3. The $\varepsilon_{r(\text{Max})}$ is measured from Fig. 4 and the E_c is measured from the same set of ceramics at about 1 kHz

maximum value in this composition range. In Fig. 8, the transition is indicated by a broad shaded line.

The phase transition sequence was also characterized by Raman spectroscopy. Figure 9 shows the Raman spectra for all compositions in this study. There were minor differences between the Raman spectra obtained from samples prepared via the conventional method (Fig. 9(a)) and the columbite method (Fig. 9(b)). Major Raman shift peaks appear at roughly 200, 262, 422, 540, 584, 698, 745, and 795 cm^{-1}, respectively. The evolution of these peaks with composition in Fig. 9 indicates the phase transition occurs at $x = 0.2$–0.3. Overall, the Raman data from the columbite prepared samples show a more distinct change between $x = 0.2$ and 0.3. The strong peaks at about 200, 540, and 745 cm^{-1} in the composition of $x = 0.1$ becomes weaker when the composition changes to $x = 0.2$. When x is further increased to 0.3 and above, these three strong peaks are smeared out. At the same time, the peak at about 795 cm^{-1} starts to emerge at $x = 0.3$ and becomes relatively strong at $x = 0.5$. The evolution of these peaks makes the whole spectrum of $x = 0.1$ and 0.2 alike and the whole spectrum of $x = 0.3$, 0.4, and 0.5 alike, respectively.

TEM examination provided supportive evidence for this phase transition sequence in the xPZN–$(1-x)$PZT system. As shown in Fig. 10, regular lamellar 90° domain configurations dominate in the tetragonal 0.1PZN–0.9PZT ceramic, while disrupted domains dominate in the rhombohedral 0.5PZN–0.5PZT ceramic with profound relaxor characteristics.

3.4. Piezoelectric properties

The effect of sintering temperature on the piezoelectric coefficient d_{33} of PZN-PZT ceramics prepared via columbite

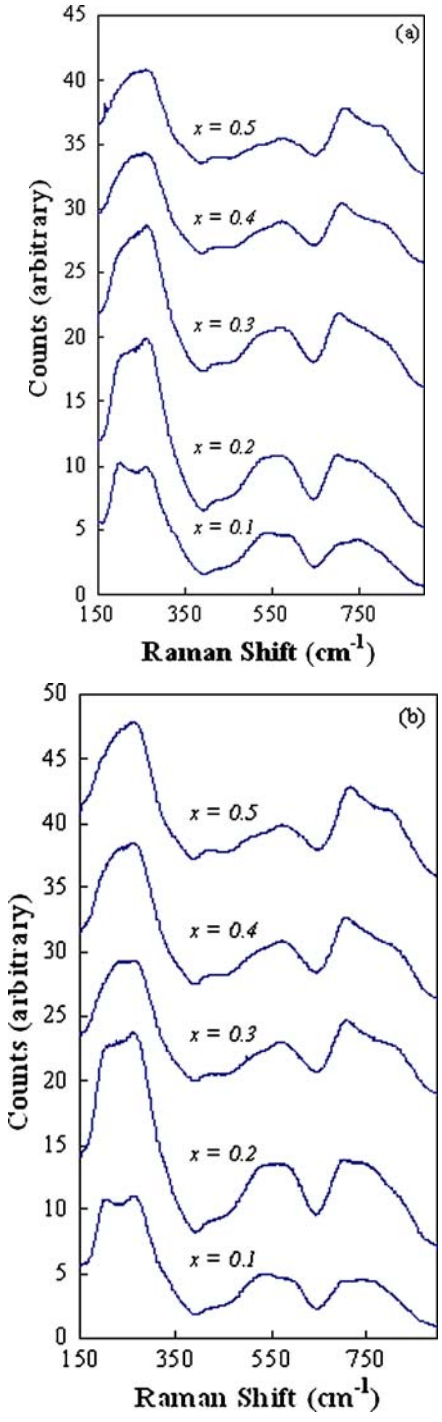

Fig. 9 Raman spectroscopy curves for xPZN–$(1-x)$PZT ceramics prepared by (a) conventional and (b) columbite methods. The ceramics were sintered at 1250°C for $x = 0.1$ and 0.2 and 1225°C for $x = 0.3$–0.5 for 2 hours

method is illustrated in Fig. 11. The coefficient d_{33} increases with increasing sintering temperature up to 1225°C and then decreases for all compositions. It is clearly apparent that the optimum processing condition is sintering at 1225°C for 2 hours. The lower d_{33} values in ceramics sintered at

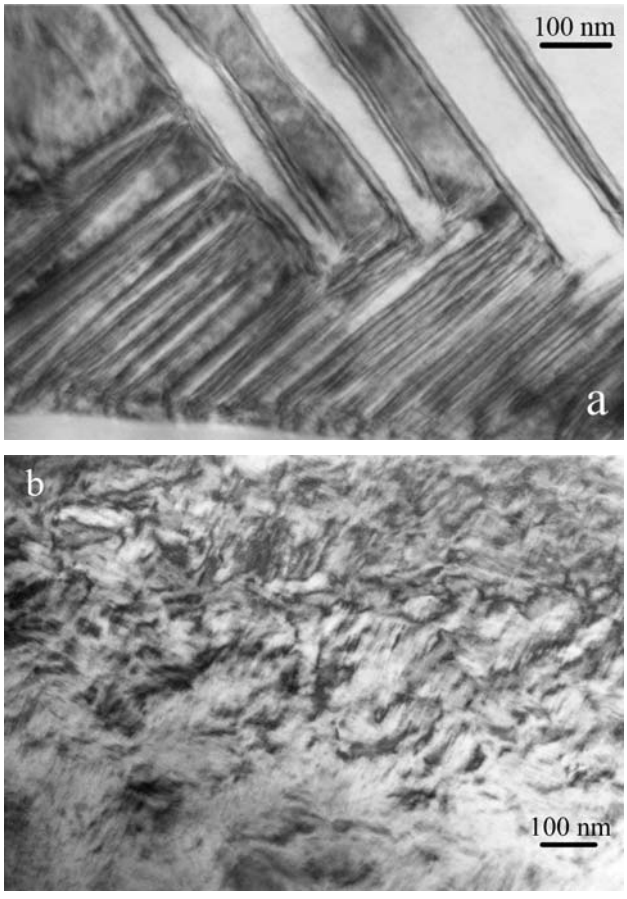

Fig. 10 TEM bright field images of ferroelectric domains in ceramics prepared by the columbite method: (a) 0.1PZN–0.9PZT ceramic sintered at 1250°C for 2 hours; and (b) the 0.5PZN–0.5PZT ceramic sintered at 1225°C for 2 hours

1250°C are presumably due to the PbO loss during the sintering process. Also evident in Fig. 11 is that the composition 0.3PZN–0.7PZT exhibits the highest piezoelectric coefficient d_{33} among all the compositions. It is interesting to note from Fig. 8 that this composition possesses a rhombohedral symmetry at room temperature and is very

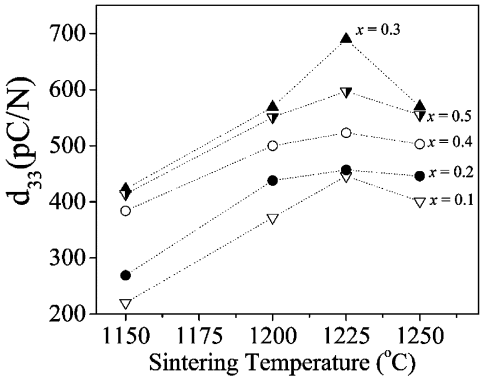

Fig. 11 Piezoelectric coefficient d_{33} as a function of sintering temperature for xPZN-$(1-x)$PZT ceramics prepared via columbite method. The duration for sintering was 2 hours

Table 2 Comparison of the piezoelectric properties observed in this study with previous studies

Ceramics	k_p (%)	d_{33}	References
$Pb(Zr_{0.53}Ti_{0.47})O_3$	52	220	[1]
$0.5PZN–0.5Pb(Zr_{0.47}Ti_{0.53})O_3$	67	430	[12]
$0.5PZN–0.5Pb(Zr_{0.5}Ti_{0.5})O_3$	67	600	Present study
$0.3PZN–0.7Pb(Zr_{0.5}Ti_{0.5})O_3$	70	690	Present study

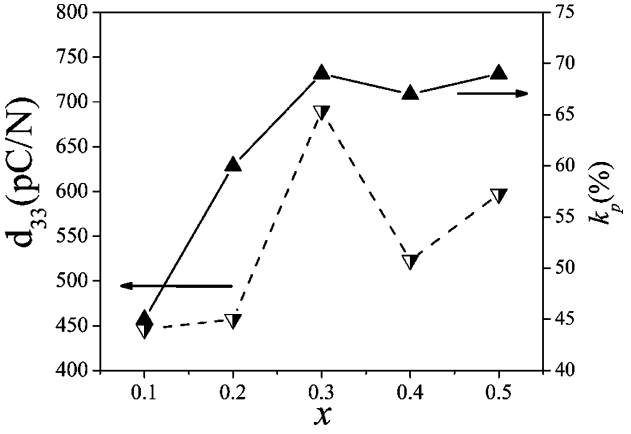

Fig. 12 Piezoelectric properties of d_{33} and k_p in ceramics prepared with the columbite method and sintered at 1250°C for $x = 0.1$–0.2 and 1225°C for $x = 0.3-0.5$ dwell 2 hours

close to the MPB. The observation is consistent with other relaxor-normal ferroelectric solid solution systems, such as the $Pb(Mg_{1/3}Nb_{2/3})$– $PbTiO_3$ and the $Pb(Zn_{1/3}Nb_{2/3})$–$PbTiO_3$ systems, where ultrahigh piezoelectric properties were found in the rhombohedral phase close to the MPB. [3, 8].

The piezoelectric coefficient d_{33} of the ceramics synthesized via the columbite method sintered at optimum conditions is replotted against the composition parameter x in Fig. 12, together with the electromechanical coupling factor k_p. High coupling factor values are noted in compositions of $x = 0.3$, 0.4 and 0.5, among which the composition 0.3PZN–0.7PZT displays the highest values. In Table 2, the piezoelectric properties observed in this study are compared with a previous study where the conventional mixed-oxide method was utilized. It is clear that ceramics with excellent piezoelectric properties can be produced in the xPZN–$(1-x)$PZT pseudo-binary system.

3.5. The PZN–PZT phase diagram

All the above results can be combined into a phase diagram which shows the complete picture of the ferroelectric $Pb(Zn_{1/3}Nb_{2/3})O_3-Pb(Zr_{0.5}Ti_{0.5})O_3$ system (Fig. 13). The data used in this phase diagram were derived from the dielectric measurements on columbite-method prepared ceramics. The two data points at $x = 0.3$ were obtained from the two peaks on the ε_r versus T curve

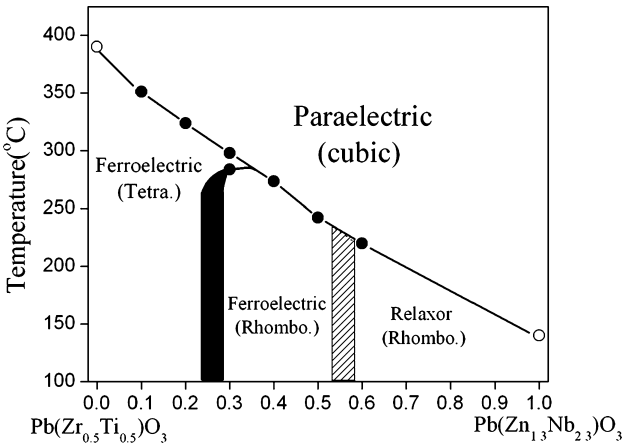

Fig. 13 The proposed phase diagram for the $Pb(Zn_{1/3}Nb_{2/3})O_3-Pb(Zr_{0.5}Ti_{0.5})O_3$ pseudo-binary solid solution system. The solid circles represent data points obtained from the present study, the open circles represent data taken from reference 1

from Fig. 5(a). According to this phase diagram, the $0.3Pb(Zn_{1/3}Nb_{2/3})O_3-0.7Pb(Zr_{0.5}Ti_{0.5})O_3$ ceramic transforms from ferroelectric rhombohedral phase to ferroelectric tetragonal phase at 283.6°C and to a paraelectric cubic phase at 298.8°C. The shaded range between $x = 0.5$ and 0.6 denotes a transition from a normal ferroelectric to a relaxor ferroelectric. As expected, the best piezoelectric properties were observed in the $0.3Pb(Zn_{1/3}Nb_{2/3})O_3-0.7Pb(Zr_{0.5}Ti_{0.5})O_3$ ceramic.

4. Conclusions

Investigations on the structure and properties of the $xPb(Zn_{1/3}Nb_{2/3})O_3-(1-x)Pb(Zr_{0.5}Ti_{0.5})O_3$ system over the range $x = 0.1-0.6$ have revealed an MPB between $x = 0.2$ and 0.3, separating a tetragonal phase from a rhombohedral phase. A normal ferroelectric to relaxor ferroelectric transition is also observed around $x = 0.5$ to 0.6. This transition corresponds to a gradual decrease in the rhombohedral distortion in the structure and a gradual increase in the frequency dispersion of the dielectric response. As expected, excellent piezoelectric properties were obtained for the $0.3Pb(Zn_{1/3}Nb_{2/3})O_3-0.7Pb(Zr_{0.5}Ti_{0.5})O_3$ composition.

Acknowledgments The authors are grateful to the Thailand Research Fund (TRF), Graduate School at Chiang Mai University and King Mongkut's Institute of Technology Ladkrabang for financial support.

References

1. B. Jaffe and W.R. Cook, *Piezoelectric Ceramic* (R.A.N. Publishers, 1971).

2. B. Noheda, D.E. Cox, G. Shirane, R. Guo, B. Jones, and L.E. Cross, *Phys. Rev. B*, **63**, 014103 (2001).
3. B. Noheda, J.A. Gonzalo, L.E. Cross, R. Guo, S.-E. Park, D.E. Cox, and G. Shirane, *Phys. Rev. B*, **61**, 8687 (2000).
4. L. Bellaiche, A. Garcia, and D. Vanderbilt, *Ferroelectrics*, **266**, 41 (2002).
5. V.A. Bokov and I.E. Myl'nikova, *Sov. Phys.-Solid State*, **3**, 631 (1961).
6. J. Kuwata, K. Uchino, and S. Nomura, *Ferroelectrics*, **37**, 579 (1981).
7. V.A. Bokov and I.E. Mylnikova, *Sov. Phys-Solid State*, **2**, 2428 (1960).
8. T.R. Shrout and A. Halliyal, *Am. Ceram. Soc. Bull.*, **66**, 704 (1987).
9. A. Halliyal, U. Kumar, R.E. Newnham, and L.E. Cross, *Am. Ceram. Soc Bull.*, **66**, 671 (1987).
10. J.R. Belsick, A. Halliyal, U. Kumar, and R.E. Newnham, *Am. Ceram. Soc. Bull.*, **66**, 664 (1987).
11. T R. Shrout, Z.P. Chang, N. Kim, and A. Markgraf, *Ferroelectr. Lett.*, **12**, 63 (1990).
12. H. Fan and H.-E. Kim, *J. Appl. Phys.*, **91**, 317 (2002).
13. N. Vittayakorn, G. Rujijanagul, T. Tunkasiri, X. Tan, and D. P. Cann, *Mat. Sci. Eng. B*, **108**, 258 (2004).
14. N. Vittayakorn, G. Rujijanagul, T. Tunkasiri, X. Tan, and D. P. Cann, *J. Mater. Res.*, **18**, 2882 (2003).
15. S.L. Swartz and T.R. Shrout, *Mater. Res. Bull.*, **17**, 1245 (1982).
16. M.-S. Yoon and H.M. Jang, *J. Appl. Phys.*, **77**, 3991 (1995).
17. K. Uchino and S. Nomura, *Ferroelectr. Lett. Sect.*, **44**, 55 (1982).